

# Implementation and application of the relativistic equation-of-motion coupled-cluster method for the excited states of closed-shell atomic systems

D. K. Nandy,<sup>\*</sup> Yashpal Singh, and B. K. Sahoo<sup>†</sup>

Theoretical Physics Division, Physical Research Laboratory, Navrangpura, Ahmedabad 380009, India

(Received 11 May 2014; published 19 June 2014)

We report the implementation of the equation-of-motion coupled-cluster (EOMCC) method in the four-component relativistic framework with a spherical atomic potential to generate the excited states from a closed-shell atomic configuration. This theoretical development will be very useful in carrying out high-precision calculations of various atomic properties in many atomic systems. We employ this method to calculate the excitation energies of many low-lying states in a few Ne-like highly charged ions, such as Cr xv, Fe xvii, Co xviii, and Ni xix ions, and compare them against their corresponding experimental values to demonstrate the accomplishment of the EOMCC implementation. The ions considered are appropriate to substantiate accurate inclusion of the relativistic effects in the evaluation of atomic properties and are also interesting for astrophysical studies. Investigation of the temporal variation of the fine-structure constant ( $\alpha$ ) obtained from astrophysical observations is a modern research problem for which we also estimate the  $\alpha$  sensitivity coefficients in the above ions.

DOI: [10.1103/PhysRevA.89.062509](https://doi.org/10.1103/PhysRevA.89.062509)

## I. INTRODUCTION

With the advent of sophisticated advanced technologies, modern research in atomic physics demands many high-precision atomic calculations. Some of the prominent examples in this context are studies of parity nonconservation (PNC) and permanent electric dipole moments (EDMs) [1,2], estimation of the uncertainties for frequency-standard measurements [3–5], probing variation of the fine-structure constant [6,7], extracting nuclear charge radii and nuclear moments [8–10], providing atomic data for astrophysical investigations [11,12] etc. In the last two decades, the coupled-cluster (CC) method for single-valence systems in the four-component relativistic framework have been extensively employed for the above-mentioned research problems with great success [13–16]. In contrast, such CC methods are less common for calculating the excited-state properties of systems with closed-shell configurations as far as the four-component relativistic approach with an explicit form of the spherical atomic potentials are concerned. There has been development of CC methods in the Fock-space formalism to calculate these states [17–19]; however, such approaches suffer from two serious problems: (i) They increase the computational complexity when applied to estimate the matrix elements of an operator and (ii) they yield an intruder-state problem while increasing the size of the model space [20]. On the other hand, the low-lying odd-parity-forbidden transitions among the singlet states of systems like Mg, Ca, Sr, Al<sup>+</sup>, In<sup>+</sup>, Hg<sup>+</sup>, Yb, etc. are considered for atomic clock experiments [21–25]. Similarly, atomic systems like Xe, Ba, Ra, Yb, Hg, Rn, etc. have been considered for PNC and EDM studies [26–31] for which high-precision calculations within the relativistic method are indispensable. Coincidentally, the excited states involved in the above research problems can be created by exciting one electron from an occupied orbital [hole (h)] to an

PACS number(s): 31.10.+z, 31.15.ag, 31.15.ap

unoccupied orbital [particle (p)] which is customarily referred to as 1h-1p excitation in the literature.

Among various popular many-body methods, equation-of-motion coupled-cluster (EOMCC) theory is one of the better suited methods to obtain the excited states [20,32]. Conceptually, the EOMCC method is identical to the linear-response coupled-cluster (LRCC) method for the calculation of the energies; however, these two approaches are quite different for the evaluation of the transition properties [33–35]. It is known that the transition moments evaluated using the EOMCC theory are not size intensive, for which a LRCC theory would be more appropriate [36]. Both the LRCC and EOMCC methods are formulated in a similar way as the excitation operators defined for the configuration-interaction (CI) method; however the excitations are carried out with respect to the exact state in contrast to the model reference state of the CI method. The uniqueness of this approach is that the energy differences between the atomic states are estimated directly by casting the Schrödinger equations in a particular form. Many nonrelativistic calculations on the ionization potentials (IPs), electron affinities (EAs), and excitation energies (EEs) in different atomic and molecular systems have been reported in the EOMCC framework [20,32,35,37–40]. Recently, this method has been developed to determine the first and second IPs of a number of closed-shell atomic systems using the atomic integrals in the four-component relativistic mechanics [41–44]. However, many of the above EOMCC calculations are carried out using molecular codes that consider special group-symmetry properties. In this work, we discuss the implementation of the EE-determining EOMCC method (referred to as the EE-EOMCC method) based on four-component relativistic mechanics and expressing the atomic potentials explicitly in spherical polar coordinates. Also, all the physical operators are represented in terms of the Racah angular momentum operators for which we make use of the reduced matrix elements in order to reduce the computational scalability.

In order to corroborate the successful implementation of the excited states determined by the EE-EOMCC method, we

<sup>\*</sup>dillip@prl.res.in

<sup>†</sup>bijaya@prl.res.in

calculate EEs of transitions among the low-lying states in a few Ne-like systems that are of immense astrophysical interest. Transition lines in the range 10.5–21.2 Å of Fe XVII are observed in the solar corona [45–48]. It is also found from observation of the stellar binary Capella that Fe XVII is one of the important constituents in the stellar corona [49], and transition lines from this ion have also been observed from various astrophysical objects by many other authors [50–55]. The above lines and transitions from Co XVIII and Ni XIX are also very important for astrophysical and tokamak plasma studies [47,56]. The reason for referring to these astrophysical observations is that the above transition lines could be potential candidates for probing temporal variation of the fine-structure constant ( $\alpha$ ). In our recent work, we have provided data to probe  $\alpha$  variation by employing a single-reference CC method formulated in the Fock-space approach for the F- and Cl-like Cr, Fe, and Ni ions [57,58]. We intend, here, to estimate the sensitivity coefficients in the considered ions for the investigation of  $\alpha$  variation; their magnitudes will gauge the significance of the relativistic effects and can be used for their detection.

## II. PERCEPTION OF $\alpha$ -VARIATION SENSITIVITY COEFFICIENTS

Probing different absorption systems associated with quasistellar objects like quasars can provide useful information regarding the speculated temporal variability of  $\alpha$ . These absorption systems that are present at different redshifts contain many metallic and nonmetallic ions of various elements. A small fraction of the absorption systems that are detected through the analysis of the quasar spectra could be intrinsically associated with the quasars themselves. Investigations of broad-absorption-line systems (BALSs) of this region reveal that the chemical compositions are usually from highly ionized species [59,60]. Next to BALSs, the most important regions are the intervening absorption systems which can be further classified into various regions depending upon the column density of neutral hydrogen (H) atoms [61–63]. The absorption lines that come out of these systems are redshifted due to the cosmological expansion of the universe and are related to the cosmological redshift parameter ( $z$ ) by the following relation:

$$\lambda_z = \lambda_{\text{rest}}(1 + z), \quad (2.1)$$

where  $\lambda_{\text{rest}}$  is the wavelength at the time of emission in the rest frame of the absorption system. With precise knowledge of the redshift of an absorption line, one can extract information about the subtle temporal variation in  $\alpha$  after cautious consideration of the systematic uncertainties associated with the observation [64]. These absorption lines are observed with advanced telescopes such as the High-Resolution Echelle Spectrograph (HIRES) at the Keck Observatory or the UV-Visual Echelle Spectrograph (UVES) at the ESO Very Large Telescope (VLT) for investigation of the variation in  $\alpha$  [65,66].

The anticipated tiny variation in  $\alpha$  from the present laboratory value  $\alpha_0$  can be inferred by combining the calculated relativistic sensitivity coefficients ( $q$ 's) of different atomic transitions with the observed spectral lines from the quasars [7]. Since the energy of an atomic level scales at the order of  $\alpha^2$  in relativistic theory, the frequency of an atomic transition

will depend on the value of  $\alpha$  at a given time. The relativistic corrections to the energy levels of a multielectron atom can be expressed as [67]

$$\Delta = -\frac{Z_a^2 (Z\alpha)^2}{2 v^3} \left( \frac{1}{J+1/2} - \frac{Z_a}{Zv} \left[ 1 - \frac{Z_a}{4Z} \right] \right), \quad (2.2)$$

where  $Z$  is the atomic number,  $J$  is the angular momentum of the state, and  $v$  and  $Z_a$  are the effective principal quantum number and effective atomic number, respectively, of an outer electron due to the screening effects of the inner core electrons. It has been shown that instead of considering two transitions from a particular atomic system [alkali-metal doublet (AD) method], it is advantageous to compare as many transitions as possible from a number of systems [many-multiplet (MM) method] to yield an order-of-magnitude improvement in the detection of change in the  $\alpha$  value ( $\Delta\alpha$ ) from observations [68–70]. Generally, one compares the measured velocity profile in the MM method to infer tiny shifts in transitions having different magnitudes of the  $q$  parameters, to obtain a stringent value of  $\frac{\Delta\alpha}{\alpha}$  from the best possible fit. In this method the change in the transition frequency between two states of an atomic system with respect to an arbitrary variation in  $\alpha$ , quantified as  $x = (\frac{\alpha}{\alpha_0})^2 - 1$ , can be given by

$$\omega(\alpha^2) \approx \omega(\alpha_0^2) + qx, \quad (2.3)$$

such that  $q = \frac{d\omega}{d(\alpha^2)}|_{x=0}$  corresponds to the rate of change of  $\omega$ , which is independent of  $x$ , and is known as the sensitivity coefficient for  $\alpha$  variation. In the MM method, the commonly used relation for the extraction of change in  $\alpha$  is given by

$$\frac{\Delta v}{c} = -\frac{2q}{\omega(\alpha_0^2)} \frac{\Delta\alpha}{\alpha}, \quad (2.4)$$

where  $c$  is the velocity of light, and  $\Delta v$  corresponds to the changes in the velocity profiles of the absorption lines that are related to the wavelengths of the atomic transitions. Therefore for probing  $\alpha$  variation using the MM method, it is imperative to find the  $q$  parameters in many possible transitions of the atomic systems that are highly abundant in astrophysical objects, like the ions considered in the present work.

## III. RELATIVISTIC ATOMIC INTEGRALS

For the present calculation, we consider following relativistic Dirac-Coulomb (DC) Hamiltonian which is rescaled with respect to the rest-mass energy of the electrons,

$$H = \sum_i \left[ c\boldsymbol{\alpha}_i \cdot \mathbf{p}_i + (\beta_i - 1)c^2 + V_{\text{nuc}}(r_i) + \sum_{j>i} \frac{1}{r_{ij}} \right], \quad (3.1)$$

where  $\boldsymbol{\alpha}_i$  and  $\beta_i$  are the usual Dirac matrices,  $V_{\text{nuc}}(r_i)$  is the nuclear potential, and  $\frac{1}{r_{ij}} = \frac{1}{|\mathbf{r}_i - \mathbf{r}_j|}$  is the interelectronic Coulombic repulsion potential. The nuclear potential is evaluated by considering the Fermi-charge distribution of the nuclear density as given by

$$\rho_{\text{nuc}}(r) = \frac{\rho_0}{1 + e^{(r-b)/d}}, \quad (3.2)$$

where the parameter  $b$  is the half charge radius as  $\rho_{\text{nuc}}(r) = \rho_0/2$  for  $r = b$ , and  $d$  is related to the skin thickness. These

parameters are evaluated by

$$d = 2.3/4(\ln 3), \quad (3.3)$$

$$b = \sqrt{\frac{5}{3}r_{\text{rms}}^2 - \frac{7}{3}d^2\pi^2} \quad (3.4)$$

with  $r_{\text{rms}}$  the root mean square radius of the nucleus.

In relativistic quantum mechanics, the four-component Dirac wave function for a single electron is expressed by

$$|\phi(r)\rangle = \frac{1}{r} \begin{pmatrix} P(r) & \chi_{\kappa,m}(\theta,\phi) \\ iQ(r) & \chi_{-\kappa,m}(\theta,\phi) \end{pmatrix}, \quad (3.5)$$

where  $P(r)$  and  $Q(r)$  are the large and small components of the wave function, respectively. The angular components have the following form:

$$\chi_{\kappa,m}(\theta,\phi) = \sum_{\sigma=\pm\frac{1}{2}} C(l\sigma j; m - \sigma, \sigma) Y_l^{m-\sigma}(\theta, \phi) \phi_\sigma \quad (3.6)$$

where  $C(l\sigma j; m - \sigma, \sigma)$  is the Clebsch-Gordan (Racah) coefficient,  $Y_l^{m-\sigma}(\theta, \phi)$  represents the normalized spherical harmonics,  $\phi_\sigma$  serves as the Pauli two-component spinors, and the relativistic quantum number  $\kappa = -(j + \frac{1}{2})a$  embodies the total and orbital quantum numbers  $j$  and  $l = j - \frac{a}{2}$ .

With the defined Dirac-Fock (DF) potential as

$$U|\phi_j\rangle = \sum_{a=1}^{\text{occ}} \langle \phi_a | \frac{1}{r_{ja}} | \phi_a \rangle |\phi_j\rangle - \langle \phi_a | \frac{1}{r_{aj}} | \phi_j \rangle | \phi_a \rangle, \quad (3.7)$$

summed over all the occupied orbitals “occ,” the DF wave function ( $|\Phi_0\rangle$ ) for a closed-shell atomic system is obtained by solving the equation

$$H_{DF}|\Phi_0\rangle = E_{DF}^{(0)}|\Phi_0\rangle, \quad (3.8)$$

which in terms of the single-particle orbitals is given by

$$\sum_i [h_0|\phi(r_i)\rangle] = \epsilon_i |\phi(r_i)\rangle \quad (3.9)$$

for the DF Hamiltonian

$$\begin{aligned} H_{DF} &= \sum_i [c\boldsymbol{\alpha}_i \cdot \mathbf{p}_i + (\beta_i - 1)c^2 + V_{\text{nuc}}(r_i) + U(r_i)] \\ &= \sum_i h_0(r_i), \end{aligned} \quad (3.10)$$

where  $h_0$  is the single-particle Fock operator.

We express  $|\phi_{n,\kappa}(r)\rangle$ , with the principal quantum number  $n$  and angular quantum number  $\kappa$ , of an electron orbital as a linear combination of Gaussian-type orbitals (GTOs) to obtain the DF orbitals. In spherical polar coordinates, it is given by

$$|\phi_{n,\kappa}(r)\rangle = \frac{1}{r} \sum_v \begin{pmatrix} C_{n,\kappa}^L N_L f_v(r) & \chi_{\kappa,m} \\ iC_{n,-\kappa}^S N_S \left(\frac{d}{dr} + \frac{\kappa}{r}\right) f_v(r) & \chi_{-\kappa,m} \end{pmatrix}, \quad (3.11)$$

where the  $C_{n,\kappa}$ 's are the expansion coefficients,  $N_{L(S)}$  are the normalization constants for the large (small) components of the wave function, and  $f_v(r) = r^l e^{-\eta_v r^2}$  are GTOs with suitably chosen parameters  $\eta_v$  for orbitals of different angular momentum symmetries. For the exponents, we use the even-tempering condition  $\eta_v = \eta_0 \zeta^{v-1}$  with two parameters  $\eta_0$

and  $\zeta$ . It can be noticed in the above expression that the large and small components of the wave function satisfy the kinetic balance condition. The orbitals are finally obtained by executing a self-consistent procedure to solve the following eigenvalue form of the DF equation:

$$\sum_v \langle f_{i,\mu} | h_0 | f_{i,v} \rangle c_{iv} = \epsilon_i \sum_v \langle f_{i,\mu} | f_{i,v} \rangle c_{iv}, \quad (3.12)$$

which is in the matrix form given by

$$\sum_v F_{\mu v} c_{iv} = \epsilon_i \sum_{\mu v} \langle f_{i,\mu} | f_{i,v} \rangle c_{iv}. \quad (3.13)$$

The above equation implies that the parity and the total angular momentum of an orbital are fixed, which are the essential conditions to describe the mechanics in spherical coordinates.

To retain the atomic spherical symmetry property in our calculations, the matrix form of the Coulomb interaction operator using the above single-particle wave functions are expressed as

$$\begin{aligned} \langle \phi_a \phi_b | \frac{1}{r_{12}} | \phi_c \phi_d \rangle &= \int dr_1 [P_a(r_1)P_c(r_1) + Q_a(r_1)Q_c(r_1)] \\ &\times \int dr_2 [P_b(r_2)P_d(r_2) + Q_b(r_2)Q_d(r_2)] \\ &\times \sum_k \frac{r_{\leq}^k}{r_{>}^{k+1}} \times F_{\text{ang}}, \end{aligned} \quad (3.14)$$

in which the  $k$  multipoles are determined by considering the triangle conditions  $|j_a - j_c| \leq k \leq j_a + j_c$  and  $|j_b - j_d| \leq k \leq j_b + j_d$  along with the additional restrictions on  $k$  obtained by multiplying with a factor  $\Pi(\kappa, \kappa', k) = \frac{1}{2}[1 - aa'(-1)^{j+j'+k}]$  that is finite only for  $l + l' + k = \text{even}$ . The angular momentum factor of the above expression is given by

$$\begin{aligned} F_{\text{ang}} &= \delta(m_a - m_c, m_d - m_b) \Pi(\kappa_a, \kappa_c, k) \Pi(\kappa_b, \kappa_d, k) \\ &\times (-1)^q \sqrt{(2j_a + 1)(2j_b + 1)(2j_c + 1)(2j_d + 1)} \\ &\times \begin{pmatrix} j_a & k & j_c \\ -m_a & q & m_c \end{pmatrix} \begin{pmatrix} j_b & k & j_d \\ -m_b & -q & m_d \end{pmatrix} \\ &\times \begin{pmatrix} j_a & k & j_c \\ \frac{1}{2} & 0 & -\frac{1}{2} \end{pmatrix} \begin{pmatrix} j_b & k & j_d \\ \frac{1}{2} & 0 & -\frac{1}{2} \end{pmatrix}, \end{aligned} \quad (3.15)$$

where  $m_j$  is the azimuthal component of  $j$ . In order to minimize the computational effort, we use the reduced matrix elements. Thus, we express

$$\begin{aligned} \langle \phi_a \phi_b | \frac{1}{r_{12}} | \phi_c \phi_d \rangle &= \delta(m_a - m_c, m_d - m_b) \sum_{k,q} \Pi(\kappa_a, \kappa_c, k) \\ &\times \Pi(\kappa_b, \kappa_d, k) (-1)^{j_a - m_a + j_b - m_b + k - q} \\ &\times \begin{pmatrix} j_a & k & j_c \\ -m_a & q & m_c \end{pmatrix} \begin{pmatrix} j_b & k & j_d \\ -m_b & -q & m_d \end{pmatrix} \\ &\times \langle ab || \frac{1}{r_{ij}} || cd \rangle, \end{aligned} \quad (3.16)$$

with the reduced matrix element

$$\begin{aligned} \langle ab || \frac{1}{r_{ij}} || cd \rangle \\ = (-1)^{j_a+j_b+k+1} \int dr_1 [P_a(r_1)P_c(r_1) + Q_a(r_1)Q_c(r_1)] \\ \times \int dr_2 [P_b(r_2)P_d(r_2) + Q_b(r_2)Q_d(r_2)] \\ \times \sqrt{(2j_a+1)(2j_b+1)(2j_c+1)(2j_d+1)} \\ \times \frac{r_{<}^k}{r_{>}^{k+1}} \begin{pmatrix} j_a & k & j_c \\ \frac{1}{2} & 0 & -\frac{1}{2} \end{pmatrix} \begin{pmatrix} j_b & k & j_d \\ \frac{1}{2} & 0 & -\frac{1}{2} \end{pmatrix}. \end{aligned} \quad (3.17)$$

#### IV. RELATIVISTIC EE-EOMCC METHOD FOR ATOMS

The starting point of our EOMCC method is the ground-state wave function ( $|\Psi_0\rangle$ ) of a closed-shell system which in the CC formalism is expressed as

$$|\Psi_0\rangle = e^T |\Phi_0\rangle, \quad (4.1)$$

where  $|\Psi_0\rangle$  is the exact ground state and  $|\Phi_0\rangle$  is the DF reference state taken in the antisymmetrized form. We have restricted consideration to only the singly and doubly excited configurations from  $|\Phi_0\rangle$  in our calculations [coupled-cluster method with single and double excitations (CCSD method)] by defining  $T = T_1 + T_2$ .  $T_1$  and  $T_2$  in the second-quantization notation are given by

$$T_1 = \sum_{a,p} a_p^\dagger a_a t_a^p \quad \text{and} \quad T_2 = \frac{1}{4} \sum_{ab,pq} a_p^\dagger a_q^\dagger a_b a_a t_{ab}^{pq}, \quad (4.2)$$

where the subscripts  $a,b$  and  $p,q$  represent the core and virtual orbitals,  $a$  and  $a^\dagger$  are the annihilation and creation operators, and  $t_a^p$  and  $t_{ab}^{pq}$  are the singly and doubly excited amplitudes. In a spherical coordinate system they are expressed as

$$\langle jm_j | T_1 | j'm'_j \rangle = (-1)^{j-m_j} \sum_{k,q} \begin{pmatrix} j & k & j' \\ -m_j & q & m'_j \end{pmatrix} \langle j || t_1^k || j' \rangle \quad (4.3)$$

and

$$\begin{aligned} \langle j_a m_a; j_b m_b | T_2 | j_c m_c; j_d m_d \rangle = & (-1)^{j_a-m_a+j_b-m_b} \\ & \times \sum_{k,q} (-1)^{k-q} \times \begin{pmatrix} j_a & k & j_c \\ -m_a & q & m_c \end{pmatrix} \\ & \times \begin{pmatrix} j_b & k & j_d \\ -m_b & -q & m_d \end{pmatrix} \langle j_a j_b || t_2^k || j_c j_d \rangle, \end{aligned}$$

where  $\langle j || t_1^k || j' \rangle$  and  $\langle j_a j_b || t_2^k || j_c j_d \rangle$  are the reduced matrix elements of the  $T_1$  and  $T_2$  operators, respectively. Owing to the nature of our orbitals, the  $T_1$  operator is scalar in our calculations but  $T_2$  will have multipoles satisfying the triangle conditions  $|j_a - j_c| \leq k \leq j_a + j_c$  and  $|j_b - j_d| \leq k \leq j_b + j_d$ . Following Eq. (3.14), it is evident that the multipoles satisfying the conditions  $j_a + j_c + k$  even and  $j_b + j_d + k$  even will be the dominant contributing multipoles. Diagrammatic representations of the  $T_1$  and  $T_2$  operators are shown in Fig. 1.

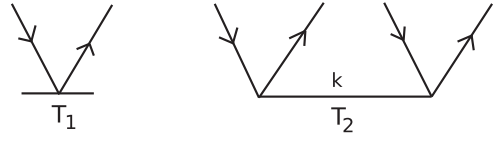


FIG. 1. Diamagnetic representations of the  $T_1$  and  $T_2$  excitation operators for the closed-shell CC method.  $k$  is the rank of the  $T_2$  operator.

The above single- and double-excitation CC amplitude equations are solved using the following matrix form:

$$\langle \Phi_0^* || H_N^{\text{eff}} \otimes T^* || \Phi_0 \rangle = 0, \quad (4.4)$$

where  $|\Phi_0^*\rangle$  corresponds to the singles ( $|\Phi_1\rangle$ ) and doubles ( $|\Phi_2\rangle$ ) excited configurations from  $|\Phi_0\rangle$  and  $H_N^{\text{eff}} = (H_N e^T)_c^{\text{op}}$  is the effective normal-ordered Hamiltonian containing only the connected ( $c$ ) open ( $op$ ) terms. Here, the  $T^*$ 's are the  $T_1$  and  $T_2$  operators in the singles and doubles amplitude-solving equations, respectively.

The excited states [ $|\Psi_K(J,\pi)\rangle$ ] having specific total angular momentum  $J$  and parity  $\pi [= (-1)^l]$  with  $l$  the orbital quantum number] from the ground state ( $|\Psi_0\rangle$ ) of a closed-shell atomic system in an EOMCC method are determined by defining an excitation operator  $\Omega_K$  as

$$|\Psi_K(J,\pi)\rangle = \Omega_K(J,\pi)|\Psi_0\rangle, \quad (4.5)$$

where  $K = 0, K = 1, K = 2$ , etc. correspond to the ground, singly excited, doubly excited, etc. states, respectively. Analogous to the CC excitation operators  $T$ , we express the  $\Omega_K$  operators in the second-quantized notation as

$$\begin{aligned} \Omega_K &= \Omega_1 + \Omega_2 + \dots \\ &= \sum_{a,p} \omega_a^p a^{p\dagger} a_a + \frac{1}{4} \sum_{ab,pq} \omega_{ab}^{pq} a^{p\dagger} a^{q\dagger} a_b a_a + \dots, \end{aligned} \quad (4.6)$$

where  $\omega_a^p$ ,  $\omega_{ab}^{pq}$ , etc. are the amplitudes of the  $\Omega_1$ ,  $\Omega_2$ , etc. operators and obviously, here,  $\Omega_0 = 1$ . Thus, the eigenvalue equations for the excited states are given by

$$\begin{aligned} H|\Psi_K\rangle &= E_K|\Psi_K\rangle, \\ H\Omega_K e^T |\Phi_0\rangle &= E_K \Omega_K e^T |\Phi_0\rangle. \end{aligned} \quad (4.7)$$

Following the second-quantization notation, we can show that  $\Omega_K$  and  $T$  commute each other. Therefore by operating with  $e^{-T}$  from the left side of the above equation, we get

$$\begin{aligned} e^{-T} H e^T \Omega_K |\Phi_0\rangle &= E_K \Omega_K |\Phi_0\rangle, \\ (e^{-T} H_N e^T + E_{DF}) \Omega_K |\Phi_0\rangle &= E_K \Omega_K |\Phi_0\rangle, \\ ((H_N e^T)_c^{\text{op}} + E_g) \Omega_K |\Phi_0\rangle &= E_K \Omega_K |\Phi_0\rangle, \end{aligned} \quad (4.8)$$

$$H_N^{\text{eff}} \Omega_K |\Phi_0\rangle = \Delta E_K \Omega_K |\Phi_0\rangle,$$

where  $E_{DF} (= \langle \Phi_0 | H | \Phi_0 \rangle)$  and  $E_g$  are the DF and ground-state energies, respectively. Therefore,  $\Delta E_K (= E_K - E_g)$  corresponds to the excitation energy of the  $|\Psi_K\rangle$  state with respect to the ground state. Using the effective Hamiltonian  $H_N^{\text{eff}}$ , we evaluate the excitation energies after projecting  $\langle \Phi_L |$  from the left-hand side to yield

$$\langle \Phi_L | H_N^{\text{eff}} \Omega_K |\Phi_0\rangle = \Delta E_K \langle \Phi_L | \Omega_K |\Phi_0\rangle \delta_{L,K}, \quad (4.9)$$

where  $|\Phi_L\rangle$  represents an excited determinantal state with definite values of  $J$  and  $\pi$ . Therefore, the  $\Omega_K$ 's have fixed  $J$  and  $\pi$  values, for which we get

$$\begin{aligned} \langle \Phi_L(J, \pi) | H_N^{\text{eff}} \Omega_K(J, \pi) | \Phi_0 \rangle \\ = \Delta E_L \langle \Phi_L(J, \pi) | \Omega_L(J, \pi) | \Phi_0 \rangle. \end{aligned} \quad (4.10)$$

By applying the completeness principle, the above equation corresponds to

$$\begin{aligned} \sum_K \langle \Phi_L(J, \pi) | H_N^{\text{eff}} | \Phi_K \rangle \langle \Phi_K | \Omega_K(J, \pi) | \Phi_0 \rangle \\ = \Delta E_L \langle \Phi_L(J, \pi) | \Omega_L(J, \pi) | \Phi_0 \rangle. \end{aligned} \quad (4.11)$$

Considering the singles ( $\Omega_1$ ) and doubles ( $\Omega_2$ ) excitations only, we write down the matrix form as

$$\begin{aligned} & \begin{pmatrix} \langle \Phi_1(J, \pi) | H_N^{\text{eff}} | \Phi_1(J, \pi) \rangle & \langle \Phi_1(J, \pi) | H_N^{\text{eff}} | \Phi_2(J, \pi) \rangle \\ \langle \Phi_2(J, \pi) | H_N^{\text{eff}} | \Phi_1(J, \pi) \rangle & \langle \Phi_2(J, \pi) | H_N^{\text{eff}} | \Phi_2(J, \pi) \rangle \end{pmatrix} \\ & \times \begin{pmatrix} \langle \Phi_1(J, \pi) | \Omega_1(J, \pi) | \Phi_0 \rangle \\ \langle \Phi_2(J, \pi) | \Omega_2(J, \pi) | \Phi_0 \rangle \end{pmatrix} \\ & = \Delta E_{1,2} \begin{pmatrix} \langle \Phi_1(J, \pi) | \Omega_1(J, \pi) | \Phi_0 \rangle \\ \langle \Phi_2(J, \pi) | \Omega_2(J, \pi) | \Phi_0 \rangle \end{pmatrix}. \end{aligned} \quad (4.12)$$

The above matrix is nonsymmetric in nature for all the finite matrix elements. We use a modified Davidson algorithm in an iterative scheme to obtain only a few roots of the lower eigenvalues, as has been applied in [71]. Unlike the  $T$  operators,  $\Omega_1$  has a finite rank equal to  $J$  of the state. Similarly,  $\Omega_2$  has an effective rank equal to  $J$  but, in contrast to the  $T_2$  operator, which is obtained from the scalar product of two equal-ranked tensor operators, the  $\Omega_2$  operators are the outcome of a general tensor product between two arbitrarily ranked tensors. Therefore, its final rank  $J$  has been determined using the following types of products:

$$\begin{aligned} \langle J_1 \pi | |[t^{k_1} u^{k_2}]^J| | J_2 \pi \rangle &= (2J+1)^{1/2} \sum_{J_3} (-1)^{J_1+J_2+J} \\ &\times \begin{Bmatrix} k_1 & k_2 & J \\ J_2 & J_1 & J_3 \end{Bmatrix} \langle J_1 \pi | |t^{k_1}| | J_3 \pi \rangle \\ &\times \langle J_3 \pi | |u^{k_2}| | J_2 \pi \rangle. \end{aligned} \quad (4.13)$$

The diagrammatic representation of the  $\Omega_K$  operators is shown in Fig. 2.

To reduce computational scalability, we divide  $H_N^{\text{eff}}$  into effective one-body, two-body, and three-body terms with two, four, and six open lines, respectively. We also make use of the

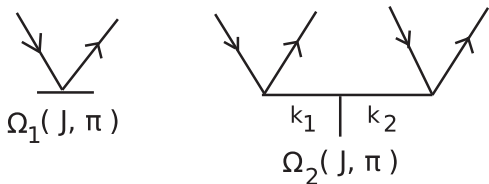


FIG. 2. Diamagnetic representations of the  $\Omega_1$  and  $\Omega_2$  EE-EOMCC excitation operators.  $J$  and  $\pi$  are the total angular momentum and parity carried by the operators. As shown, the  $J$  value of the  $\Omega_2$  operator is determined following a triangular condition among two other operators having ranks  $k_1$  and  $k_2$ .

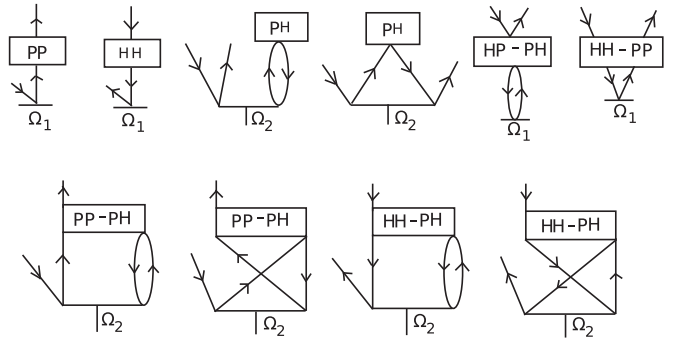


FIG. 3. EE-EOMCC diagrams to determine the amplitudes of the  $\Omega_1$  operators.

effective two-body terms to construct the effective three-body terms. Using these diagrams the final contributing diagrams used to calculate amplitudes for the  $\Omega_1$  and  $\Omega_2$  operators are shown in Figs. 3 and 4, respectively.

## V. RESULTS AND DISCUSSION

To obtain well-behaved single-particle orbitals, we have taken suitable values of the parameters  $\eta_0$  and  $\zeta$  along with sufficiently large numbers of GTOs for different angular momentum symmetries. For the CC calculations, however, we consider only the the orbitals (active orbitals) that contribute significantly within the precision of our interest. All the information regarding the considered basis set is provided in Table I. As seen from the table, we have not considered orbitals from the  $g$  symmetry onwards. Since the systems are highly contracted due to ionization and we are interested only in the calculations of the low-lying states of the considered systems, contributions from the higher-symmetry orbitals are expected to be small.

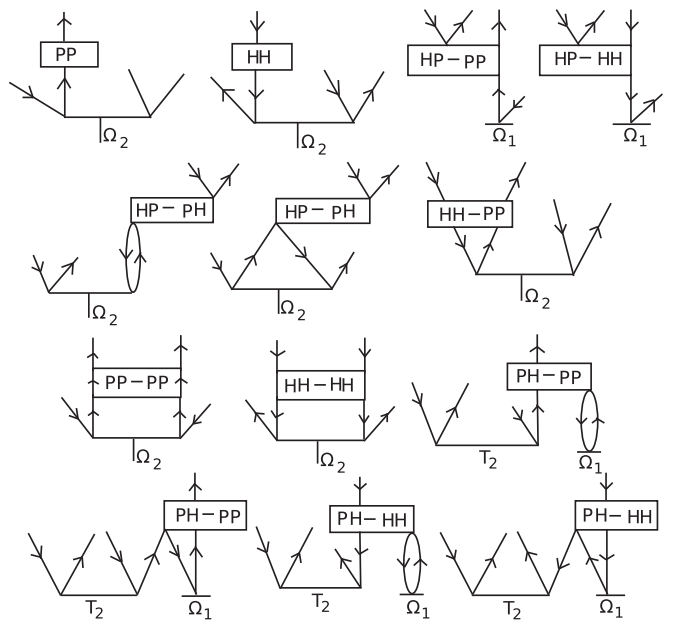


FIG. 4. EE-EOMCC diagrams to determine the amplitudes of the  $\Omega_2$  operators.

TABLE I. Details of the basis functions considered for all the ions.

	<i>s</i>	<i>p</i>	<i>d</i>	<i>f</i>
Parameters				
$\eta_0$	0.00625	0.00638	0.00654	0.00667
$\zeta$	2.03	2.07	2.19	2.27
No. of GTOs	35	34	33	32
Active orbitals	13	12	10	8

We employ the developed relativistic EE-EOMCC method to calculate energies for many low-lying excited states of the Cr XV, Fe XVII, Co XVIII, and Ni XIX ions with different values of the total angular momentum and odd parity. The calculated energies at the CCSD level are reported and compared against the values listed in the NIST database [72] in Table II. In order to realize the role of the correlation effects incorporated through the CCSD method, we take the approximation in the effective Hamiltonian as  $H_N^{\text{eff}} \equiv H_N$  and obtain the EEs in the equation-of-motion framework. These results are quoted as second-order many-body perturbation theory [MBPT(2) method] results in the same table. We also give EEs estimated from the orbital energies in the same table as the DF results.

As seen from Table II, EEs obtained using the DF method are overestimated compared with the experimental results listed in the NIST database and the MBPT(2) results are underestimated for all the calculated states in the considered ions. Our CCSD results and the values from NIST are in close agreement and the differences between them are quoted in terms of a percentage as  $\Delta$  in the above table. From the  $\Delta$  values, it is clear that the percentages of the accuracies in our calculations are subdecimal in all cases.

Among the theoretical calculations, the most recent one was carried out by Aggarwal *et al.* in which they employed the multiconfigurational Dirac-Fock (MCDF) method using the general-purpose relativistic atomic structure package (GRASP) [73] to calculate the energies along with other properties of the Fe XVII ion [74]. Their calculated energies are found to be underestimated in all the considered excited states compared to the NIST data. Bhatia *et al.* calculated some of these energies in Fe XVII using a superstructure (ss) code in a semirelativistic approach considering the Breit-Pauli Hamiltonian [75], but their results, when compared with the NIST data, are slightly overestimated and less accurate than our CCSD results. Further, Cornille *et al.* also evaluated these energy levels along with a few more states using the same ss code [76], but their estimated energies are undervalued compared with the NIST results. In another work, Sampson *et al.* obtained the excitation energies in the Fe XVII ion using a Dirac-Fock-Slater (DFS) atomic code [77] and their results follow a similar trend as obtained by Bhatia *et al.* As compared to others, our CCSD results for the EEs in the Fe XVII ion are in close agreement with the values given in the NIST database. However, we have not found calculations of EEs in other ions using relativistic methods to make a comparative study. Nevertheless, the excellent agreement between our CCSD results and the experimental values compared with calculations carried out using other methods demonstrates the potential of

the EE-EOMCC method to produce accurate results for the excited states in the closed-shell ions considered.

After achieving high-precision calculations of the energies for many transitions in the ions considered, we intend now to estimate the relativistic sensitivity coefficients  $q$  for all these transitions. In the Fe XVII ion, we have determined the  $q$  parameters for 25 possible intercombination transitions that are given in Table III. Among them three transitions  $2s^2 2p^5 3s\ 3P_2^o \rightarrow 2s^2 2p^5 3s\ 1P_1^o$ ,  $2s^2 2p^5 3d\ 3P_0^o \rightarrow 2s^2 2p^5 3d\ 3P_2^o$ , and  $2s^2 2p^5 3d\ 3P_1^o \rightarrow 2s^2 2p^5 3d\ 3P_2^o$  lie in the optical regime with the wavelengths 6544.50, 4460.30, and 6849.31 Å, respectively. There are also two transitions  $2s^2 2p^5 3s\ 3P_0^o \rightarrow 2s^2 2p^5 3s\ 3P_1^o$  and  $2s^2 2p^5 3d\ 3P_0^o \rightarrow 2s^2 2p^5 3d\ 3P_1^o$  that lie in the near-infrared regime while the rest of the transitions fall within the ultraviolet (UV) to the extreme ultraviolet (EUV) regions of the electromagnetic spectrum. It is worth mentioning that the spectra of the Fe XVII ion have been extensively studied by many astrophysics groups for investigating different astrophysical plasmas and solar plasmas, and also in the observation of the absorption lines coming from various quasars like IRAS 13349 + 2438 that are detected by the XMM-Newton observatory [50]. Therefore, the above-estimated  $q$  parameters will serve as useful ingredients if the astrophysical observations in these lines are directed towards probing temporal variation of the fine-structure constant. For completeness in the understanding of the numerical results for the estimation of the  $q$  parameters, we also present the EEs as  $\omega(+0.025)$  and  $\omega(-0.025)$  in the same table for two different values of  $x$ , +0.025 and -0.025, referring to two different values of  $\alpha$ . The remarkable findings from these results are that we obtain large  $q$  parameters with opposite signs in different transitions which is, in fact, a very useful criterion to enhance the effect indicating the variation in  $\alpha$  from the observations of these atomic spectra. By analyzing the results of the  $q$  parameters in the Fe XVII ion one can find that there are three transitions which could be used as anchor lines, whose wavelengths are insensitive to the variation of  $\alpha$ , and transitions having large  $q$  parameters can be used as probe lines, whose wavelengths are highly sensitive to variation of  $\alpha$  [78]. The  $q$  values for these possible anchor lines are -1660, -758, and 1364 cm<sup>-1</sup>, whose corresponding laboratory wavelengths lie in the EUV, optical, and near infrared (NIR) domains of the electromagnetic spectrum. Observations of these EUV lines from any absorption system will be redshifted towards the optical range of the spectrum, which could be easily detected using an earth-based observatory. Similarly, we estimate the  $q$  parameters for 15 possible transitions in the Co XVIII ion and present them in Table III. Unlike the case of Fe XVII, the considered transition frequencies in the Co XVIII ion lie only in the UV range. For Co XVIII we find five transition with positive  $q$  values and the remaining ten transitions correspond to negative  $q$  values. Among all the transitions in Co XVIII we can choose the  $2s^2 2p^6\ 1S_0 \rightarrow 2s^2 2p^5 3d\ 3P_1^o$  transition as an anchor line because of its small  $q$  value.

In Table III, we report the results for the  $\alpha$  sensitivity coefficients for the Cr XV and Ni XIX ions. For both these ions, we have considered 25 possible transitions to estimate the  $q$  parameters. In the case of Cr XV, the transition  $2s^2 2p^5 3d\ 3P_0^o \rightarrow 2s^2 2p^5 3d\ 3P_2^o$  lies in the optical region whereas all other transitions fall in the UV range. Out

TABLE II. Absolutes values of the excitation energies (in cm<sup>-1</sup>) of a few low-lying states in the Cr xv, Fe xvii, Co xviii, and Ni xix ions.

State	Term	<i>J</i>	Others	This work			NIST	$\Delta$
				DF	MBPT(2)	CCSD		
<b>Cr xv</b>								
$2s^2 2p^6$	$^1S_0$	0		0	0	0	0	
$2s^2 2p^5 3s$	$^3P_2^o$	2		5076633	4700197	4711049	4714294	0.06
	$^1P_1^o$	1		5076633	4717618	4728787	4727500	0.03
$2s^2 2p^5 3s$	$^3P_0^o$	0		5150041	4773037	4783974	4784174	0.004
	$^3P_1^o$	1		5150041	4786118	4796971	4793200	0.07
$2s^2 2p^5 3d$	$^3P_0^o$	0		5666530	5241502	5252079	5253448	0.03
	$^3P_1^o$	1		5666530	5250734	5261208	5259419	0.03
$2s^2 2p^5 3d$	$^3P_2^o$	2		5666530	5263315	5273858	5270945	0.05
<b>Fe xvii</b>								
$2s^2 2p^6$	$^1S_0$	0	0	0	0	0	0	
$2s^2 2p^5 3s$	$^3P_2^o$	2	5833877.08 <sup>a</sup> 5852291.01 <sup>b</sup> 5838683.58 <sup>c</sup> 5852261.00 <sup>d</sup>	6252544	5837409	5846872	5849490	0.04
	$^1P_1^o$	1	5849646.34 <sup>a</sup> 5868334.60 <sup>b</sup> 5854891.78 <sup>c</sup> 5868270.00 <sup>d</sup>	6252544	5856420	5866053	5864770	0.02
$2s^2 2p^5 3s$	$^3P_0^o$	0	5935877.92 <sup>a</sup> 5952931.10 <sup>b</sup> 5943131.56 <sup>c</sup> 5953692.00 <sup>d</sup>	6358361	5942319	5951894	5951210	0.01
	$^3P_1^o$	1	5945710.38 <sup>a</sup> 5963268.35 <sup>b</sup> 5953699.26 <sup>c</sup> 5964194.00 <sup>d</sup>	6358361	5955899	5965332	5960870	0.07
$2s^2 2p^5 3d$	$^3P_0^o$	0	6448998.63 <sup>a</sup> 6468773.30 <sup>b</sup> 6454156.28 <sup>c</sup> 6466891.00 <sup>d</sup>	6930674	6454603	6463808	6463980	0.002
	$^3P_1^o$	1	6456855.82 <sup>a</sup> 6476685.35 <sup>b</sup> 6462628.00 <sup>c</sup> 6475529.00 <sup>d</sup>	6930674	6465750	6474902	6471800	0.05
$2s^2 2p^5 3d$	$^3P_2^o$	2	6471845.94 <sup>a</sup> 6491971.76 <sup>b</sup> 6478035.12 <sup>c</sup> 6491737.00 <sup>d</sup>	6930674	6481571	6490752	6486400	0.07
<b>Co xviii</b>								
$2s^2 2p^6$	$^1S_0$	0		0	0	0	0	
$2s^2 2p^5 3s$	$^3P_1^o$	1		6885258	6468217	6482537	6477900	0.07
$2s^2 2p^5 3s$	$^1P_1^o$	1		7010851	6587125	6601429	6592400	0.13
$2s^2 2p^5 3d$	$^3P_1^o$	1		7608386	7116091	7130032	7122000	0.11
$2s^2 2p^5 3d$	$^3D_1^o$	1		7612379	7206635	7219885	7210800	0.12
$2s^2 2p^5 3d$	$^1P_1^o$	1		7733980	7331833	7343682	7334600	0.12
<b>Ni xix</b>								
$2s^2 2p^6$	$^1S_0$	0		0	0	0	0	
$2s^2 2p^5 3s$	$^3P_2^o$	2		7547742	7093993	7102363	7105260	0.04
	$^1P_1^o$	1		7547742	7114641	7123258	7122600	0.01
$2s^2 2p^5 3s$	$^3P_0^o$	0		7695794	7240746	7249098	7247700	0.02
	$^3P_1^o$	1		7695794	7254858	7263159	7258100	0.07

TABLE II. (Continued.)

State	Term	<i>J</i>	Others	This work			
				DF	MBPT(2)	CCSD	NIST
$2s^2 2p^5 3d$	$^3P_0^o$	0		8316575	7789854	7797906	7797965
	$^3P_1^o$	2		8316575	7822402	7830453	7847100
	$^3P_2^o$	1		8316575	7803113	7811208	7807700

<sup>a</sup>Reference [74].<sup>b</sup>Reference [75].<sup>c</sup>Reference [77].<sup>d</sup>Reference [76].TABLE III. Sensitivity  $q$  coefficients (in cm<sup>-1</sup>) for the Fe XVII and Co XVIII ions using the CCSD method. The frequencies  $\omega(+0.025)$  and  $\omega(-0.025)$  are given as absolute values.

Transitions	$J_f$	$\lambda$ (Å)	$\omega(+0.025)$	$\omega(-0.025)$	$q$
<b>Fe XVII</b>					
$2s^2 2p^6 \ ^1S_0 \rightarrow 2s^2 2p^5 3s \ ^3P_0^o$	2	17.09	5845928	5847815	-37747
$\rightarrow 2s^2 2p^5 3s \ ^1P_1^o$	1	17.05	5865127	5866977	-36989
$\rightarrow 2s^2 2p^5 3s \ ^3P_1^o$	1	16.77	5967034	5963673	67235
$\rightarrow 2s^2 2p^5 3d \ ^3P_1^o$	1	15.45	6474858	6474941	-1660
$\rightarrow 2s^2 2p^5 3d \ ^3P_2^o$	2	15.41	6490842	6490653	-3795
$2s^2 2p^5 3s \ ^3P_2^o \rightarrow 2s^2 2p^5 3s \ ^1P_1^o$	1	6544.50	19199	19162	-758
$\rightarrow 2s^2 2p^5 3s \ ^3P_0^o$	0	983.09	107655	102338	-106347
$\rightarrow 2s^2 2p^5 3s \ ^3P_1^o$	1	897.83	121106	115857	-104982
$\rightarrow 2s^2 2p^5 3d \ ^3P_0^o$	0	162.73	617721	616148	-31456
$\rightarrow 2s^2 2p^5 3d \ ^3P_2^o$	1	160.69	628930	627126	-36086
$\rightarrow 2s^2 2p^5 3d \ ^3P_2^o$	2	157.00	644914	642837	-41542
$2s^2 2p^5 3s \ ^1P_1^o \rightarrow 2s^2 2p^5 3s \ ^3P_0^o$	0	1156.87	88455	83176	-105589
$\rightarrow 2s^2 2p^5 3s \ ^3P_1^o$	1	1040.58	101906	96695	-104224
$\rightarrow 2s^2 2p^5 3d \ ^3P_0^o$	0	166.73	598521	596986	-30698
$\rightarrow 2s^2 2p^5 3d \ ^3P_1^o$	1	164.73	609730	607964	-35328
$\rightarrow 2s^2 2p^5 3d \ ^3P_2^o$	2	160.16	625714	623675	-40784
$2s^2 2p^5 3s \ ^3P_0^o \rightarrow 2s^2 2p^5 3s \ ^3P_1^o$	1	10351.97	13451	13519	1364
$\rightarrow 2s^2 2p^5 3d \ ^3P_1^o$	1	192.09	521275	524788	70260
$\rightarrow 2s^2 2p^5 3d \ ^3P_2^o$	2	186.85	537259	540499	64805
$2s^2 2p^5 3s \ ^3P_1^o \rightarrow 2s^2 2p^5 3d \ ^3P_0^o$	0	198.76	496614	500290	73526
$\rightarrow 2s^2 2p^5 3d \ ^3P_1^o$	1	195.72	507823	511268	68896
$\rightarrow 2s^2 2p^5 3d \ ^3P_2^o$	2	190.28	523808	526980	63440
$2s^2 2p^5 3d \ ^3P_0^o \rightarrow 2s^2 2p^5 3d \ ^3P_1^o$	1	12787.72	11209	10978	-4630
$\rightarrow 2s^2 2p^5 3d \ ^3P_2^o$	2	4460.30	27193	26689	-10085
$2s^2 2p^5 3d \ ^3P_1^o \rightarrow 2s^2 2p^5 3d \ ^3P_2^o$	2	6849.31	15984	15711	-5455
<b>Co XVIII</b>					
$2s^2 2p^6 \ ^1S_0 \rightarrow 2s^2 2p^5 3s \ ^3P_0^o$	1	15.43	6481449	6483622	-43460
$\rightarrow 2s^2 2p^5 3s \ ^1P_1^o$	1	15.16	6603472	6599388	81684
$\rightarrow 2s^2 2p^5 3d \ ^3P_1^o$	1	14.04	7130003	7130057	-1081
$\rightarrow 2s^2 2p^5 3d \ ^3D_1^o$	1	13.86	7220232	7219522	14193
$\rightarrow 2s^2 2p^5 3d \ ^1P_1^o$	1	13.63	7346134	7341253	97615
$2s^2 2p^5 3s \ ^3P_1^o \rightarrow 2s^2 2p^5 3s \ ^1P_1^o$	1	873.36	122023	115765	-125145
$\rightarrow 2s^2 2p^5 3d \ ^3P_1^o$	1	155.25	648554	646435	-42379
$\rightarrow 2s^2 2p^5 3d \ ^3D_1^o$	1	136.44	738783	735900	-57653
$\rightarrow 2s^2 2p^5 3d \ ^1P_1^o$	1	116.72	864684	857630	-141076
$2s^2 2p^5 3s \ ^1P_1^o \rightarrow 2s^2 2p^5 3d \ ^3P_1^o$	1	188.82	526530	530669	82766
$\rightarrow 2s^2 2p^5 3d \ ^3D_1^o$	1	161.70	616759	620134	67491
$\rightarrow 2s^2 2p^5 3d \ ^1P_1^o$	1	134.73	742661	741864	-15931
$2s^2 2p^5 3d \ ^3P_1^o \rightarrow 2s^2 2p^5 3d \ ^3D_1^o$	1	1126.12	90229	89465	-15274
$\rightarrow 2s^2 2p^5 3d \ ^1P_1^o$	1	470.36	216130	211195	-98697
$2s^2 2p^5 3d \ ^3D_1^o \rightarrow 2s^2 2p^5 3d \ ^1P_1^o$	1	807.75	125901	121730	-83422

TABLE IV. Sensitivity  $q$  coefficients (in  $\text{cm}^{-1}$ ) for the Cr xv and Ni xix ions using the CCSD method. The frequencies  $\omega(+0.025)$  and  $\omega(-0.025)$  are given as absolute values.

Transitions	$J_f$	$\lambda (\text{\AA})$	$\omega(+0.025)$	$\omega(-0.025)$	$q$
<b>Cr xv</b>					
$2s^2 2p^6 \ ^1S_0 \rightarrow 2s^2 2p^5 3s \ ^3P_2^o$	2	21.21	4710372	4711725	-27045
$\rightarrow 2s^2 2p^5 3s \ ^1P_1^o$	1	21.15	4727989	4729293	-26088
$\rightarrow 2s^2 2p^5 3s \ ^3P_1^o$	1	20.86	4798109	4795838	45409
$\rightarrow 2s^2 2p^5 3d \ ^3P_1^o$	1	19.01	5261218	5261286	-1342
$\rightarrow 2s^2 2p^5 3d \ ^3P_2^o$	2	18.97	5273946	5273762	3676
$2s^2 2p^5 3s \ ^3P_2^o \rightarrow 2s^2 2p^5 3s \ ^1P_1^o$	1	7572.31	17616	17568	-956
$\rightarrow 2s^2 2p^5 3s \ ^3P_0^o$	0	1431.02	74775	71106	-73375
$\rightarrow 2s^2 2p^5 3s \ ^3P_1^o$	1	1267.33	87736	84113	-72454
$\rightarrow 2s^2 2p^5 3d \ ^3P_0^o$	0	185.47	541564	540494	-21406
$\rightarrow 2s^2 2p^5 3d \ ^3P_2^o$	1	183.44	550845	549560	-25702
$\rightarrow 2s^2 2p^5 3d \ ^3P_2^o$	2	179.64	563573	562037	-30721
$2s^2 2p^5 3s \ ^1P_1^o \rightarrow 2s^2 2p^5 3s \ ^3P_0^o$	0	1764.48	57158	53537	-72418
$\rightarrow 2s^2 2p^5 3s \ ^3P_1^o$	1	1522.07	70119	66545	-71498
$\rightarrow 2s^2 2p^5 3d \ ^3P_0^o$	0	190.13	523947	522925	-20450
$\rightarrow 2s^2 2p^5 3d \ ^3P_1^o$	1	187.99	533229	531992	-24746
$\rightarrow 2s^2 2p^5 3d \ ^3P_2^o$	2	184.01	545957	544468	-29765
$2s^2 2p^5 3s \ ^3P_0^o \rightarrow 2s^2 2p^5 3s \ ^3P_1^o$	1	11079.10	12961	13007	920
$\rightarrow 2s^2 2p^5 3d \ ^3P_1^o$	1	210.42	476070	478454	47672
$\rightarrow 2s^2 2p^5 3d \ ^3P_2^o$	2	205.43	488798	490931	42653
$2s^2 2p^5 3s \ ^3P_1^o \rightarrow 2s^2 2p^5 3d \ ^3P_0^o$	0	217.27	453827	456380	51048
$\rightarrow 2s^2 2p^5 3d \ ^3P_1^o$	1	214.49	463109	465447	46752
$\rightarrow 2s^2 2p^5 3d \ ^3P_2^o$	2	209.31	475837	477923	41732
$2s^2 2p^5 3d \ ^3P_0^o \rightarrow 2s^2 2p^5 3d \ ^3P_1^o$	1	16747.61	9281	9066	-4296
$\rightarrow 2s^2 2p^5 3d \ ^3P_2^o$	2	5715.26	22009	21543	-9315
$2s^2 2p^5 3d \ ^3P_1^o \rightarrow 2s^2 2p^5 3d \ ^3P_2^o$	2	8676.03	12727	12476	-5019
<b>Ni xix</b>					
$2s^2 2p^6 \ ^1S_0 \rightarrow 2s^2 2p^5 3s \ ^3P_2^o$	2	14.07	7100997	7103565	-51360
$\rightarrow 2s^2 2p^5 3s \ ^1P_1^o$	1	14.03	7121845	7124365	-50388
$\rightarrow 2s^2 2p^5 3s \ ^3P_1^o$	1	13.78	7265582	7260715	97342
$\rightarrow 2s^2 2p^5 3d \ ^3P_1^o$	2	12.74	7830543	7830327	4309
$\rightarrow 2s^2 2p^5 3d \ ^3P_2^o$	1	12.80	7811084	7811160	-1520
$2s^2 2p^5 3s \ ^3P_2^o \rightarrow 2s^2 2p^5 3s \ ^1P_1^o$	1	5767.01	20848	20799	-971
$\rightarrow 2s^2 2p^5 3s \ ^3P_0^o$	0	702.05	150566	143087	-149579
$\rightarrow 2s^2 2p^5 3s \ ^3P_1^o$	1	654.27	164585	157150	-148703
$\rightarrow 2s^2 2p^5 3d \ ^3P_0^o$	0	144.36	696739	694506	-44658
$\rightarrow 2s^2 2p^5 3d \ ^3P_2^o$	2	134.80	729545	726762	-55669
$\rightarrow 2s^2 2p^5 3d \ ^3P_2^o$	1	142.36	710086	707594	-49840
$2s^2 2p^5 3s \ ^1P_1^o \rightarrow 2s^2 2p^5 3s \ ^3P_0^o$	0	799.36	129718	122288	-148607
$\rightarrow 2s^2 2p^5 3s \ ^3P_1^o$	1	738.00	143736	136350	-147731
$\rightarrow 2s^2 2p^5 3d \ ^3P_0^o$	0	148.07	675891	673706	-43686
$\rightarrow 2s^2 2p^5 3d \ ^3P_1^o$	2	138.02	708697	705962	-54698
$\rightarrow 2s^2 2p^5 3d \ ^3P_2^o$	1	145.96	689238	686794	-48868
$2s^2 2p^5 3s \ ^3P_0^o \rightarrow 2s^2 2p^5 3s \ ^3P_1^o$	1	9615.38	14018	14062	876
$\rightarrow 2s^2 2p^5 3d \ ^3P_1^o$	2	166.83	578979	583674	93909
$\rightarrow 2s^2 2p^5 3d \ ^3P_2^o$	1	178.57	559520	564506	99739
$2s^2 2p^5 3s \ ^3P_1^o \rightarrow 2s^2 2p^5 3d \ ^3P_0^o$	0	185.23	532154	537356	104044
$\rightarrow 2s^2 2p^5 3d \ ^3P_1^o$	2	169.78	564960	569612	93033
$\rightarrow 2s^2 2p^5 3d \ ^3P_2^o$	1	181.95	545501	550444	98862
$2s^2 2p^5 3d \ ^3P_0^o \rightarrow 2s^2 2p^5 3d \ ^3P_1^o$	2	2035.21	32806	32255	-11011
$\rightarrow 2s^2 2p^5 3d \ ^3P_2^o$	1	10272.21	13347	13088	-5182
$2s^2 2p^5 3d \ ^3P_1^o \rightarrow 2s^2 2p^5 3d \ ^3P_2^o$	1	2538.07	19459	19167.72	5829

of 25 considered transitions in Cr xv, eight have positive and the rest have negative  $q$  values as given in Table IV. In this ion, the largest positive and negative  $q$  parameters correspond to the transitions  $2s^2 2p^5 3s\ 3P_1^o \rightarrow 2s^2 2p^5 3d\ 3P_0^o$  and  $2s^2 2p^5 3s\ 3P_2^o \rightarrow 2s^2 2p^5 3d\ 3P_0^o$ , respectively. Finally, we also present the results for the Ni xix ion in Table IV. Similar to the case of Cr xv, Ni xix ion also has one optical transition  $2s^2 2p^5 3s\ 3P_2^o \rightarrow 2s^2 2p^5 3s\ 3P_1^o$  and rest of the transitions fall in the UV region. The  $q$  values in this ion have similar trends to those in Cr xv. We have nine positive and 16 negative  $q$  coefficients with the largest positive and negative  $q$  values as 104 044 cm<sup>-1</sup> and -149 579 cm<sup>-1</sup>, respectively.

Analogously to the Fe xvii ion, the possible anchor lines in the case of Cr xv correspond to wavelengths 19.01, 7572.31, and 11 079.10 Å with the  $q$  values -1342, -956, and 920, cm<sup>-1</sup>, respectively. Moreover in the Ni xix ion, the transitions  $2s^2 2p^6 1S_0 \rightarrow 2s^2 2p^5 3d\ 3P_2^o$ ,  $2s^2 2p^5 3s\ 3P_2^o \rightarrow 2s^2 2p^5 3s\ 1P_1^o$ , and  $2s^2 2p^5 3s\ 3P_0^o \rightarrow 2s^2 2p^5 3s\ 3P_1^o$  which lie in the EUV, optical, and NIR regions, respectively, have small  $q$  values and can be chosen as the anchor lines.

## VI. CONCLUSION

We have implemented an equation-of-motion coupled-cluster method to calculate the excited states of a closed-shell atomic system in a four-component relativistic framework that preserves spherical symmetric properties explicitly. The method has been employed to calculate the excitation energies

of four different highly charged ions that are of astrophysical interest. Our calculations are very accurate as compared to their corresponding experimental values. The development will be very useful for studying a variety of atomic properties of many atomic systems for which high-precision calculations are in demand. The present method can adequately address the roles of the relativistic and the electron correlation effects scrupulously to achieve high-precision results to clarify many physical problems of modern research interest. To illustrate its potential application, we employ the above method to calculate excitation energies for different values of the fine-structure constant in a number of transitions in the considered ions and estimate the relativistic sensitivity coefficients which are of great interest in the investigation of temporal variation of the fine-structure constant using the laboratory astrophysics method. We found large sensitivity coefficients of opposite signs that may be very useful to be analyzed for the detection of enhanced drifts in the course of searching for possible variation in the fine-structure constant.

## ACKNOWLEDGMENTS

We are grateful to B. P. Das and D. Mukherjee for many useful discussions on the theory during the implementation of the code. We thank M. Kallay for providing us the diagonalization program used in the code to obtain lower roots of a nonsymmetric matrix. The calculations were carried out using the PRL 3TFLOP HPC cluster, Ahmedabad.

- 
- [1] J. S. M. Ginges and V. V. Flambaum, *Phys. Rep.* **397**, 63 (2004).
  - [2] M. Pospelov and A. Ritz, *Ann. Phys. (N.Y.)* **318**, 119 (2005).
  - [3] J. L. Hall, *Rev. Mod. Phys.* **78**, 1279 (2006).
  - [4] T. W. Hänsch, *Rev. Mod. Phys.* **78**, 1297 (2006).
  - [5] D. J. Wineland, *Rev. Mod. Phys.* **85**, 1103 (2013).
  - [6] J. P. Uzan, *Rev. Mod. Phys.* **75**, 403 (2003).
  - [7] H. Chand, R. Srianand, P. Petitjean, B. Aracil, R. Quast, and D. Reimers, *Astron. Astrophys.* **451**, 45 (2006).
  - [8] M. G. H. Gustavsson and Ann-Marie Mrtensson-Pendrill, in *Handbook of Molecular Physics and Quantum Chemistry*, edited by S. Wilson, (Wiley, New York, 2003), Vol. 1, Part 6, Chap. 30, p. 477.
  - [9] L. W. Wansbeek, S. Schlessler, B. K. Sahoo, A. E. L. Dieperink, C. J. G. Onderwater, and R. G. E. Timmermans, *Phys. Rev. C* **86**, 015503 (2012).
  - [10] M. Avgoulea *et al.*, *J. Phys. G* **38**, 025104 (2011).
  - [11] A. Ivanchik *et al.*, *Astron. Astrophys.* **440**, 45 (2005).
  - [12] J. A. King, M. T. Murphy, W. Ubachs, and J. K. Webb, *Mon. Not. R. Astron. Soc.* **417**, 3010 (2011).
  - [13] B. K. Sahoo, B. P. Das, and D. Mukherjee, *Phys. Rev. A* **79**, 052511 (2009).
  - [14] B. K. Sahoo, Md. R. Islam, B. P. Das, R. K. Chaudhuri, and D. Mukherjee, *Phys. Rev. A* **74**, 062504 (2006).
  - [15] Y. Singh, D. K. Nandy, and B. K. Sahoo, *Phys. Rev. A* **86**, 032509 (2012).
  - [16] B. Arora, D. K. Nandy, and B. K. Sahoo, *Phys. Rev. A* **85**, 012506 (2012).
  - [17] E. Eliav, U. Kaldor, and Y. Ishikawa, *Phys. Rev. A* **52**, 291 (1995).
  - [18] A. Borschevsky, V. Pershina, E. Eliav, and U. Kaldor, *Phys. Rev. A* **87**, 022502 (2013).
  - [19] B. K. Mani and D. Angom, *Phys. Rev. A* **83**, 012501 (2011).
  - [20] I. Shavitt and R. J. Bartlett, *Many-Body Methods in Chemistry and Physics* (Cambridge University Press, New York, 2009).
  - [21] S. A. Diddams *et al.*, *Science* **293**, 825 (2001).
  - [22] P. Gill *et al.*, *Meas. Sci. Technol.* **14**, 1174 (2003).
  - [23] P. Gill, *Metrologia* **42**, S125 (2005).
  - [24] T. Rosenband *et al.*, *Phys. Rev. Lett.* **98**, 220801 (2007).
  - [25] T. Rosenband *et al.*, *Science* **319**, 1808 (2008).
  - [26] C. S. Wood *et al.*, *Science* **275**, 1759 (1997).
  - [27] V. A. Dzuba, V. V. Flambaum, and J. S. M. Ginges, *Phys. Rev. D* **66**, 076013 (2002).
  - [28] W. C. Griffith, M. D. Swallows, T. H. Loftus, M. V. Romalis, B. R. Heckel, and E. N. Fortson, *Phys. Rev. Lett.* **102**, 101601 (2009).
  - [29] M. A. Rosenberry and T. E. Chupp, *Phys. Rev. Lett.* **86**, 22 (2001).
  - [30] K. V. P. Latha, D. Angom, B. P. Das, and D. Mukherjee, *Phys. Rev. Lett.* **103**, 083001 (2009).
  - [31] Y. Singh, B. K. Sahoo, and B. P. Das, *Phys. Rev. A* **89**, 030502(R) (2014).
  - [32] P. Piecuch and R. J. Bartlett, *Adv. Quantum Chem.* **34**, 295 (1999).
  - [33] H. J. Monkhorst, *Int. J. Quantum Chem.* **12**, 421 (1977).
  - [34] E. Dalgaard and H. J. Monkhorst, *Phys. Rev. A* **28**, 1217 (1983).

- [35] D. Mukherjee and P. K. Mukherjee, *Chem. Phys.* **39**, 325 (1979).
- [36] H. Koch, R. Kobayashi, A. S. de Merás, and P. Jørgensen, *J. Chem. Phys.* **100**, 4393 (1994).
- [37] J. F. Stanton and R. J. Bartlett, *J. Chem. Phys.* **98**, 7029 (1993).
- [38] J. R. Gour, P. Piecuch, and M. Wloch, *Int. J. Quantum Chem.* **106**, 2854 (2006).
- [39] M. Hubert, L. K. Sørensen, J. Olsen, and T. Fleig, *Phys. Rev. A* **86**, 012503 (2012).
- [40] M. Hubert, J. Olsen, J. Loras, and T. Fleig, *J. Chem. Phys.* **139**, 194106 (2013).
- [41] M. Das, R. K. Chaudhuri, S. Chattopadhyay, U. S. Mahapatra, and P. K. Mukherjee, *J. Phys. B* **44**, 165701 (2011).
- [42] R. K. Chaudhuri, *Int. J. Mol. Sci.* **4**, 586 (2003).
- [43] H. Pathak, B. K. Sahoo, B. P. Das, N. Vaval, and S. Pal, *Phys. Rev. A* **89**, 042510 (2014).
- [44] H. Pathak, A. Ghosh, B. K. Sahoo, B. P. Das, N. Vaval, and S. Pal, *Phys. Rev. A* **89**, 042510 (2014).
- [45] B. Edlén and F. Tyrén, *Z. Phys.* **101**, 206 (1936).
- [46] F. Tyrén, *Z. Phys.* **111**, 314 (1938).
- [47] M. Klapisch *et al.*, *Phys. Lett. A* **69**, 34 (1978).
- [48] D. L. McKenzie and P. B. Landecker, *Astrophys. J.* **254**, 309 (1982).
- [49] M. Audard *et al.*, *Astron. Astrophys.* **365**, L329 (2001).
- [50] M. Sako *et al.*, *Astron. Astrophys.* **365**, L168 (2001).
- [51] C. Jupén, *Mon. Not. R. Astr. Soc.* **208**, 1P (1984).
- [52] K. P. Dere, *Astrophys. J.* **221**, 1062 (1978).
- [53] U. Feldman, G. A. Doscheck, and J. F. Seely, *Mon. Not. R. Astr. Soc.* **212**, 41P (1985).
- [54] A. K. Dupree, N. S. Brickhouse, G. A. Doscheck, J. C. Green, and J. C. Raymond, *Astrophys. J.* **418**, L41 (1993).
- [55] J. K. Lepson *et al.*, LLNL Report No. CONF-574833, 2012 (unpublished).
- [56] U. Feldman, L. Cohen, and M. Swartz, *Astrophys. J.* **148**, 585 (1967).
- [57] D. K. Nandy and B. K. Sahoo, *Phys. Rev. A* **88**, 052512 (2013).
- [58] D. K. Nandy and B. K. Sahoo, *Astron. Astrophys.* **563**, A25 (2014).
- [59] E. Behar, M. Sako, M. Steven, and M. Kahn, *Astrophys. J.* **563**, 497 (2001).
- [60] P. J. Green *et al.*, *Astrophys. J.* **558**, 109 (2001).
- [61] J. X. Prochaska, J. C. Howk, and A. M. Wolfe, *Nature (London)* **423**, 57 (2003).
- [62] A. M. Wolfe, D. A. Turnshek, H. E. Smith, and R. D. Cohen, *Astrophys. J. Suppl.* **61**, 249 (1986).
- [63] W. L. W. Sargent, C. C. Steidel, and A. Boksenberg, *Astrophys. J. Suppl.* **69**, 703 (1989).
- [64] P. Molaro *et al.*, *Astron. Astrophys.* **555**, A68 (2013).
- [65] S. A. Levshakov, M. Centurión, P. Molaro, and S. D'Odorico, *Astron. Astrophys.* **434**, 827 (2005).
- [66] M. T. Murphy, J. K. Webb, and V. V. Flambaum, *Mon. Not. R. Astron. Soc.* **384**, 1053 (2008).
- [67] V. A. Dzuba, V. V. Flambaum, and J. K. Webb, *Phys. Rev. A* **59**, 230 (1999).
- [68] V. A. Dzuba, V. V. Flambaum, and J. K. Webb, *Phys. Rev. Lett.* **82**, 888 (1999).
- [69] M. T. Murphy *et al.*, in *Astrophysics, Clocks and Fundamental Constants*, edited by S. G. Karshenboim and E. Peik, Lecture Notes in Physics Vol. 648 (Springer-Verlag, Berlin, 2004), p. 131.
- [70] S. A. Levshakov, in *Astrophysics, Clocks and Fundamental Constants* (Ref. [69]), p. 151.
- [71] Y. J. Bomble, J. C. Saeh, J. F. Stanton, P. G. Szalay, M. Kállay, and J. Gauss, *J. Chem. Phys.* **122**, 154107 (2005).
- [72] <http://physics.nist.gov/cgi-bin/ASD/energy1.pl>
- [73] I. P. Grant, B. J. McKenzie, P. H. Norrington, D. F. Mayers, and N. C. Pyper, *Comput. Phys. Commun.* **21**, 207 (1980).
- [74] K. M. Aggarwal, F. P. Keenan, and A. Z. Msezane, *Astrophys. J. Suppl.* **144**, 169 (2003).
- [75] A. K. Bhatia and J. L. R. Saba, *Astrophys. J.* **563**, 434 (2001).
- [76] M. Cornille *et al.*, *Astron. Astrophys. Suppl. Ser.* **105**, 77 (1994).
- [77] D. H. Sampson, H. L. Zhang, A. K. Mohanty, and R. E. H. Clark, *Phys. Rev. A* **40**, 604 (1989).
- [78] M. G. Kozlov, V. A. Korol, J. C. Berengut, V. A. Dzuba, and V. V. Flambaum, *Phys. Rev. A* **70**, 062108 (2004).